Supplementary materials

S1. Numerical stability of COMSOL model

The Courant number is a dimensionless parameter that indicates the number of mesh cells an information traversed during a specific timestep. As a results, if the Courant number is superior to one, the simulated information might skip a neighbour cell (SIMSCALE, 2020). Therefore, to ensure the stability of the solution, it is recommended to keep this parameter inferior to one. The courant number is defined by:

$$C = \frac{q \times \Delta t}{\Delta x}$$

With q the groundwater flux, Δt the computational time step and Δx the size of the mesh cell. In this study, Δt = 300 s, Δx = 0.0185 m and the maximal flux q estimated from passive-DTS data interpretation is 3.10×10^{-5} m.s^{-1}. As a result, the Courant number is equal to:

$$C = \frac{3.10 \times 10^{-5} \times 300}{0.0185} = 0.5$$

which is inferior to 1, ensuring the numerical stability of the solution.

S2. Punctual in-situ measurement of infiltration rates

This section describes point-scale infiltration measurements conducted in shallow wells within the loess sediments of the study site using the Porchet method (Colombani *et al.*, 1973), a widely used borehole infiltration test for estimating infiltration rates. This method determines infiltration by monitoring the rate at which water infiltrates from a borehole under a constant head, considering both lateral seepage through the borehole walls and vertical infiltration through the bottom. The test consists of maintaining a steady water level in a pre-drilled borehole while recording the infiltrated volume over time. Figure S1 illustrates the setup for one of the boreholes.

The infiltration rate is computed using the following equation (Colombani *et al.*, 1973) and accounts for lateral seepage.

$$Infiltration\ rate = \frac{V}{dt \times (2\pi \times r \times \frac{h_1 + h_2}{2} + S)}$$

Where V is the infiltrated volume, dt is the time interval between two successive measurements, S is the cross-sectional area of the well, r is the borehole radius and h_1 and h_2 are the water heights at the beginning and end of the time interval, respectively.

The infiltration rates obtained using this method represent initial infiltration rates and are therefore comparable to those inferred from passive-DTS analysis. Measurements were conducted in three wells: one inside the infiltration basin and two outside, all located within the loess sediments. Initially, a 5-minute refilling period was used, but this was later extended to 15 minutes to minimize errors associated with water height readings.

Results for the three measurement boreholes are depicted in Figure S2. The obtained infiltration rates of 1.12×10^{-5}, 1.25×10^{-5} and 1.50×10^{-5} m.s^{-1} are of the same order of magnitude as the mean infiltration rate of 1.51×10^{-5} m.s^{-1} derived from passive-DTS analysis.

Figure S1. Porchet method illustrated in a shallow well within loess sediments.

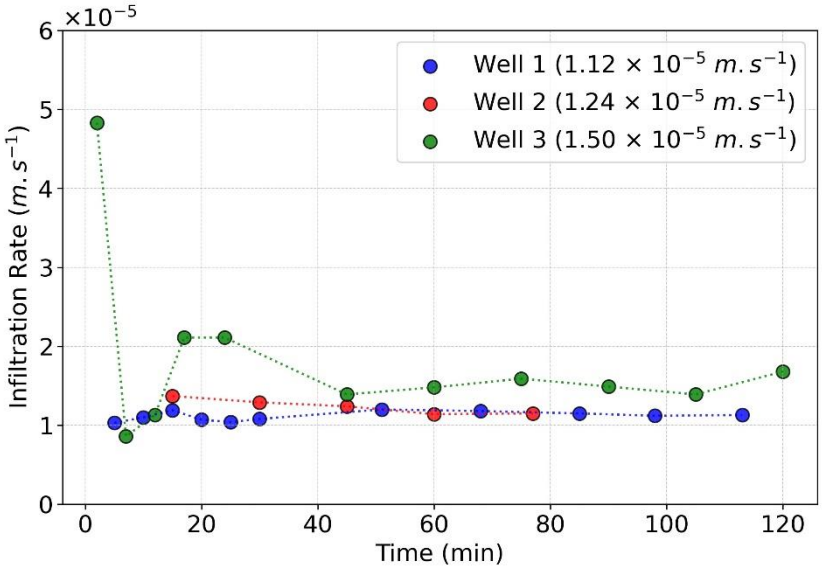

Figure S2. Results from the Porchet method for three shallow boreholes in loess sediments. The written values represent the mean infiltration rate. Note that for well 3, the average value was calculated after the fifth measurement to allow for the stabilization of the rate.

S3. Input parameters for the heat transfer model in COMSOL

The purpose of this section is to clarify the origin and calculation of all parameters presented in Table 1 of the main manuscript. COMSOL requires the thermal properties of the solid grains within the sediments, rather than those of the saturated medium. Therefore, the following calculations utilize equations from the COMSOL 'Heat Transfer' module user manual (COMSOL, 2018) to derive the thermal properties of the solid grains from the properties of the saturated medium and the fluid flowing through it. For clarity, we have modified the indices used in the manual: the indices 'eff,' 's,' and 'w' refer to the saturated medium, solid, and water, respectively.

Density and porosity

In parallel with the granulometric analysis, the bulk density of the solid grains was measured and determined to be ρ_s = 2700 kg m^{-3}. Similarly, the density of water is universally recognized as ρ_w = 1000 kg m^{-3}.

The total porosity of loess materials was determined through granulometry analysis, yielding a value of Θ = 0.42. Consequently, the solid fraction is calculated as Θ_s = 1 - Θ = 0.58.

Thermal conductivity

The thermal conductivity of water, denoted as λ_w is sourced from Stauffer *et al.* (2013) and has a value of 0.58 $W.m^{-1}.K^{-1}$. The mean thermal conductivity of the saturated porous media, also named effective thermal conductivity, was determined from active-DTS data analysis, yielding a value of λ_{eff} = 1.78 W m^{-1} K^{-1}. Using the equation provided in the COMSOL 'Heat Transfer' module user manual (COMSOL, 2018), we derived the thermal conductivity of the solid materials λ_s.

$$\lambda_{eff} = \theta_s\lambda_s + (1-\theta_s)\lambda_w$$

$$\lambda_s = \frac{\lambda_{eff} - (1-\theta_s)\lambda_w}{\theta_s}$$

$$\lambda_s = \frac{1.78 - (1-0.58)0.58}{0.58} = 2.65\ W\ m^{-1}\ s^{-1}$$

Heat capacity

The volumetric heat capacity of water is sourced from Stauffer *et al.* (2013) and has a value of $\rho_w C_w$ = 4.1 × 10^6 J m^{-3} K^{-1}. Similarly, the volumetric heat capacity of saturated porous loess can be approximated to that of saturated loam, yielding a value of $(\rho C)_{eff}$ = 3 × 10^6 J m^{-3} K^{-1} (Bilskie, 1994; Khaled A and Nidal H, 2020). Using the relationships and equations provided in the COMSOL 'Heat Transfer' module user manual (COMSOL, 2018), we derived the heat capacity of the solid materials.

$$(\rho C)_{eff} = \theta_s\rho_s C_s + (1-\theta_s)\rho_w C_w$$

$$C_s = \frac{(\rho C)_{eff} - (1-\theta_s)\rho_w C_w}{\theta_s\rho_s} = \frac{3 \times 10^6 - (1-0.58) \times 4.1 \times 10^6}{0.58 \times 2700} = 816\ J\ kg^{-1}K^{-1}$$

And the volumetric heat capacity of the solid matrix is given by :

$$\rho_s C_s = 816 \times 2700 = 2.2\ MJ\ m^{-3}K^{-1}$$

S4. Temperature evolution over space

In line with the specified methodology outlined in the section 2, temperature data were systemically collected along the entire length of the FO cable throughout the experimental period. Figure S3 illustrates distinct temperature profiles observed along the FO cable at different stages of the study. Starting from the DTS unit, the cable transits a hot calibration bath (Hot CB) spanning 8.5 and 16.5 m, attaining temperatures of up to 38°C. Subsequently, upon exiting the hot CB for a brief distance, the FO cable encounters the cold calibration bath (Cold CB) within the range of 27.5 to 38 m, resulting in temperatures approximately at 1°C. Following traversal through both calibration baths, the FO cable proceeds towards the infiltration basin, initiating its underground trajectory within loess sediments spanning 57.75 to 75.25 m, with temperatures around 16°C before the replenishment of the basin (Figure S3A), corresponding to the ambient temperature of the superficial loess at that juncture. However, once the basin is filled with water, temperatures recorded along the buried section of the FO cable are maintained around 14°C, corresponding to the temperature of the recharge water (Figure S3B and Figure S3C). On day 4, within this buried segment, the section between 67.25 and 74.25 m of

the cable is subject to electrical heating, resulting in an increase of temperature up to 27-28°C (Figure S3C). On the same day, immediately after emerging from the loess sediments, the FO cable revisits the aforementioned cold calibration bath, recording a return to cold temperatures approximating 0 to 1°C. Out of the sections of the FO cable previously mentioned, temperatures recorded along the FO cable reflect ambient atmospheric conditions prevalent on the experimental day, ranging between 18-20°C. Instances of lower temperatures, such as 14°C before and after the underground traverse through the loess sediments, are attributed to the shading effects induced by the infiltration basin sides, thereby protecting those cable sections from direct solar radiation exposure.

The section of interest in which thermal responses will be studied more accurately corresponds to the buried section within the infiltration basin since it is this particular segment that will be subjected to groundwater flow during the infiltration test. The thermal responses across the entire length of this section will be examined for passive DTS data analysis. In the context of active DTS data analysis, focus will be exclusively on the thermal responses from the electrically heated segment.

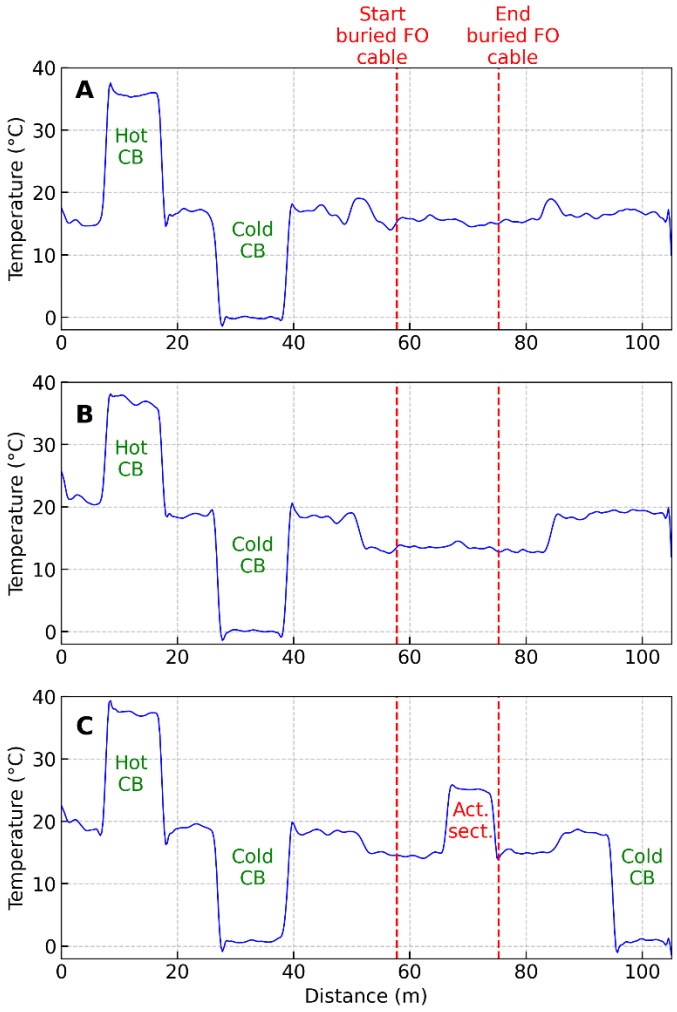

Figure S3. Calibrated temperature evolution along the FO cable before the basin replenishment (A), after the basin replenishment (B) and during the heating of a FO cable section (C).

S5. Thermal conductivity measurement in laboratory

To compare the estimated thermal conductivity values from active-DTS data analysis, a needle probe method was applied in laboratory. The thermal conductivity of the loess was measured using a needle probe method. This method involves inserting a needle into a soil sample placed in a cylindrical

container. The needle acts as a known heat source at the center of the container, and the thermal conductivity transmitted by the sample is measured using a thermocouple in the probe.

Loess samples were collected from the bottom of the infiltration basin and saturated by mixing with water to replicate conditions similar to those during the infiltration test. The saturated sample was then placed in a cylindrical container, and a needle probe was inserted into the sample, as illustrated in Figure S4.

Figure S4. Needle probe measurement method of thermal conductivity on saturated loess sample.

The thermal response over time was recorded and is presented in Figure S5 and the thermal conductivity (λ) was determined using the following equation (Fourteau *et al.*, 2022) during the conduction dominant stage:

$$\lambda = \frac{q}{4\pi \times \Delta T} \Delta \ln(t)$$

With λ is the thermal conductivity, T is the temperature and t the time. The heat input q is defined as $q = \frac{I^2 R}{L}$ where R and L represent the resistance and length of the probe, respectively, and I is the current supplied to the heating resistor. A thermal conductivity of 1.55 $W.m^{-1}.K^{-1}$ was measured from the saturated loess sample. This value is slightly lower than the field measurements; however, these results should be interpreted with caution, as laboratory conditions differ from those in the field. In particular, the degree of compaction within the cylindrical container influences the measurement, and it is challenging to determine the level of compaction that best represents in situ conditions.

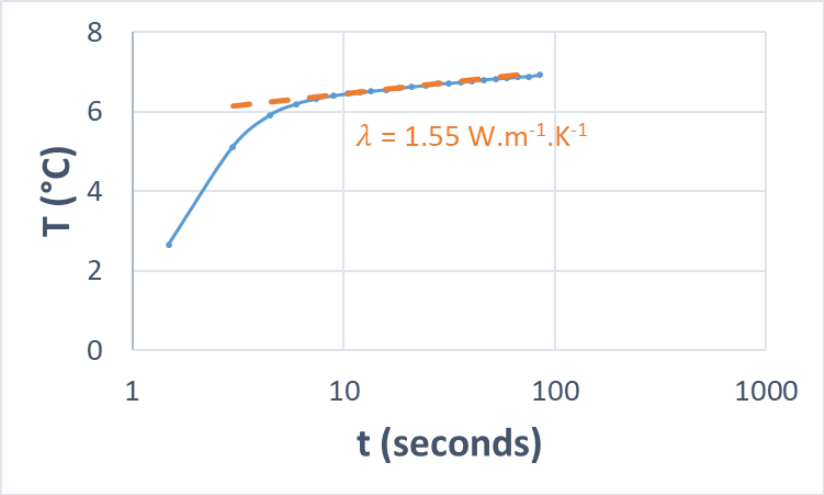

Figure S5. Thermal response obtained using the thermal needle probe (blue) and associated analytical thermal conductivity model (dashed orange).

S6. Thermal Peclet number calculation

This section provides a detailed calculation of the thermal Peclet number, which is crucial for understanding the sensitivity of the heat transfer model used for interpreting passive-DTS data. A thermal Peclet number greater than one indicates that heat transfer is dominated by advection rather than conduction. As discussed in the main text, the thermal Peclet number helps explain why thermal conductivity has a relatively low impact on the interpretation of passive-DTS measurements, particularly during the initial stages of infiltration where advection dominates over conduction.

As mentioned by Anderson (2005), the Peclet number is a dimensionless number that represents the ratio of advection to dispersion, used in solute transport and heat transfer studies. As such, the thermal Peclet number has been calculated in the case of the sensitivity analysis for passive-DTS data interpretation to understand the low sensitivity of thermal conductivity in the heat transfer model developed in COMSOL. The thermal Peclet number is given by:

$$\mathrm{Pe} = \frac{\rho_w c_w q L}{\lambda_e} = \frac{4.2 \times 10^6 \times 1.05 \times 10^{-5} \times 0.1}{1.78} = 2.48$$

With $\rho_w c_w$ = 4.2 × 10^6 J.m^{-3}.K^{-1} the volumetric heat capacity of the water, λ_e = 1.78 W.m^{-1}.K^{-1} the effective thermal conductivity, q = 1.05 × 10^{-5} m.s^{-1} the seepage velocity and L = 0.1 m the characteristic length.

Bibliography

[1] Bilskie, J.R. (1994) *Dual probe methods for determining soil thermal properties: numerical and laboratory study*. Doctor of Philosophy. Iowa State University, Digital Repository. Available at: https://doi.org/10.31274/rtd-180813-11719.

[2] Colombani, J., Lamagat, J.-P. and Thiebaux, J. (1973) 'MESURE DE LA PERMÉABILITÉ DES SOLS EN PLACE: UN NOUVEL APPAREIL POUR LA MÉTHODE MUNTZ UNE EXTENSION DE LA MÉTHODE PORCHET AUX SOLS HÉTÉROGÈNES', *Hydrological Sciences Bulletin*, 18(2), pp. 197–235. Available at: https://doi.org/10.1080/02626667309494027.

[3] COMSOL (2018) *Heat Transfer Module User's Guide, Version 5.4*. Available at: https://doc.comsol.com/5.4/doc/com.comsol.help.heat/HeatTransferModuleUsersGuide.pdf (accessed 13th march 2025).

[4] Fourteau, K. *et al.* (2022) 'On the use of heated needle probes for measuring snow thermal conductivity', *Journal of Glaciology*, 68(270), pp. 705–719. Available at: https://doi.org/10.1017/jog.2021.127.

[5] Khaled A, A. and Nidal H, A.-H. (2020) 'Specific Heat and Volumetric Heat Capacity of Some Saudian Soils as affected by Moisture and Density', *International Journal of Materials*, 7. Available at: https://doi.org/10.46300/91018.2020.7.8.

[6] SIMSCALE (2020) 'What is a Courant Number?'. https://www.simscale.com/knowledge-base/what-is-a-courant-number (Accessed 11 November 2024).